Magnetic susceptibility and EPR measurements in concentrated spin-glasses: $Cd_{1-x}Mn_xTe$ and $Cd_{1-x}Mn_xSe$

S. B. Oseroff
Centro de Física, Instituto Venezolano de Investigaciones Científicas, Apartado 1827, Caracas 1010A, Venezuela

(Received 30 March 1981; revised manuscript received 19 February 1982)

We have measured the magnetic susceptibility and the electron paramagnetic resonance for $Cd_{1-x}Mn_xTe$ ($0.001 \leq x \leq 0.60$) and $Cd_{1-x}Mn_xSe$ ($0.001 \leq x \leq 0.45$) as a function of magnetic field, temperature, time, and microwave frequency. For $x < 0.20$, both systems remain paramagnetic for all temperatures measured ($0.7 \leq T \leq 300$ K). Above $x \simeq 0.20$, a cusp in the low-field susceptibility after zero-field cooling was observed at a temperature T_f, its position being a linear function of concentration. A broadening and a shift in the magnetic field of the electron paramagnetic resonance line with decreasing temperature were observed, and found to be independent of the microwave frequency used (9 and 35 GHz). The isothermal remanent and thermoremanent magnetization were studied in detail. The magnetic properties of these systems are similar to those of the canonical metallic spin-glasses, with the exception that the scaling law for the magnetization is not obeyed.

I. INTRODUCTION

The existence and characteristics of spin-glass regimes in diluted solutions of transition ions in metallic matrices have been the subject of many experimental[1] and theoretical[2] investigations in the last few years. However, it is still an open question whether the temperature T_f of the sharp cusp observed in the zero-field susceptibility[3] marks the presence of a new kind of phase transition.[4] The nature of this phase transition, and indeed its very existence, remains in doubt.

In metallic spin-glasses, it is not always easy to separate the contribution of the conduction electrons from that of the localized moments, for instance, in the case of specific heat (C_p).[5] For a better understanding of spin-glasses, it would be useful to study simpler systems which also show a spin-glass behavior. It has been suggested by De Seze,[6] and discussed by Villain,[7] that the best way to obtain an insulating spin-glass is to use frustrated disordered systems with only antiferromagnetic (AF) interactions. Good candidates for this purpose are mixed crystals formed by the substitution of transition-metal ions in II-VI semiconductors. $Cd_{1-x}Mn_xTe$ and $Cd_{1-x}Mn_xSe$ belong to this group of materials, known as magnetic semiconductors. Because of their large electronic energy gaps, these systems behave like insulators at low temperature, and consequently there is no Rudderman-Kittel-Kasuya-Yosida (RKKY) interaction between the spins. If a spin-glass behavior is observed in these systems it must be explained by a mechanism in which the interaction is predominantly short ranged.

$Cd_{1-x}Mn_xTe$ forms a zinc-blende structure for $0 \leq x \leq 0.70$ in which the Mn atoms randomly replace Cd atoms in an fcc sublattice. $Cd_{1-x}Mn_xSe$ has a wurtzite structure for $0 \leq x \leq 0.50$, where the Mn^2 and Cd^{2+} randomly occupy an hcp sublattice. The Mn ions interact only antiferromagnetically in these substances. A spin-glass phase with only AF interactions was predicted for an fcc lattice due to frustration.[6,7] A similar behavior can be expected for an hcp arrangement.

Preliminary data of these materials indicate that we can distinguish two different regions of Mn concentration (x).[8] For $x < 0.20$, the system remains paramagnetic for all T measured. Above $x \simeq 0.20$, we measured a cusp in the low field χ after zero-field cooling (ZFC). These observations motivated us to do a systematic study of the magnetic properties of these systems. To achieve this we performed magnetic susceptibility (χ) and electron paramagnetic resonance (EPR) measurements through a wide range of Mn concentrations as a function of magnetic field (H), temperature (T), time (t) and microwave frequency (ν), in order to arrive to a better understanding of the similarities and differences in the magnetic behavior between

these materials and metallic spin-glasses. Recently, Galazka *et al.*[9] reported data on C_p and low-field χ measurements in $Cd_{1-x}Mn_xTe$, concluding that this system behaves as a spin-glass for $0.2 \leq x <= 0.6$.

The format of this paper is as follows. In Sec. II experimental procedures are presented. In Sec. III we present our experimental results. In Sec. IV we analyze the experimental results and finally, the discussion and conclusions are given in Sec. V.

II. EXPERIMENTAL TECHNIQUES

Good quality single crystals, up to $x=0.60$ and 0.45, were prepared using a modified Bridgman technique for $Cd_{1-x}Mn_xTe$ and $Cd_{1-x}Mn_xSe$, respectively. Composition and homogeneity of the samples were analyzed by atomic absorption and density measurements. The measured composition agreed well with the nominal concentration.

The measurements of the magnetization (M) as a function of H and T were made using the Faraday method in the range $1 \leq H \leq 10$ kOe and $0.7 \leq T \leq 300$ K, and a vibrating sample magnetometer system for $0.03 < H < 6$ kOe and $1.5 \leq T \leq 25$ K. The EPR data were obtained using Varian spectrometers operating at 9 and 35 GHZ for $1.5 \leq T \leq 300$ K. T was determined either from the vapor pressure of the liquid surrounding the sample or from suitably calibrated resistors.

To measure the remanent magnetization (M_R) as a function of t, H, T, and x, we used two different techniques. One set of data was obtained using the vibrating magnetometer. Another was obtained by a simple EPR technique that allows us to obtain simultaneously the M and the normal EPR data.[10] This was possible by gluing two thin phosphorus-doped silicon EPR markers to the sample which was polished to a rectangular prismatic shape. The markers were placed on the adjacent faces of the prism, with one marker facing the magnet poles. The M data were obtained by measuring the separation between the two EPR marker signals as a function of T, x, and time t. Typical linewidths of the silicon-doped markers were ~ 0.3 Oe for $T \lesssim 25$ K.

III. EXPERIMENTAL RESULTS

A. dc susceptibility

Our data for the inverse susceptibility χ^{-1} vs T for $Cd_{1-x}Mn_xTe$ and $Cd_{1-x}Mn_xSe$ are shown in Figs. 1 and 2. We observe that for $x \geq 0.20$, χ depends on whether or not the sample is cooled in an external field. When the sample is cooled at zero field, a maximum in $\chi(T)$ is observed at a temperature T_f which depends on x and H. The susceptibility measured at 30 Oe for field-cooled (FC) and ZFC samples is given in Fig. 3. When H is increased, the maximum became weaker, broader, and shifted to lower temperatures. The values of T_f as a function of H, after ZFC, are given in Fig. 4 for both systems.

B. EPR results

The EPR spectra have been studied at 9 and 35 GHz between 1.5 and 300 K for $0.001 \leq x \leq 0.60$ in $Cd_{1-x}Mn_xTe$ and $0.001 \leq x \leq 0.45$ for $Cd_{1-x}Mn_xSe$. At room temperature the spectrum was almost independent of frequency for both systems. At $x < 0.005$ a well-resolved hyperfine structure was observed in agreement with previous results.[11,12] For $x > 0.005$ the hyperfine lines initially broaden due to the dipole-dipole interaction, eventually becoming a single broad line for $x \sim 0.015$. The linewidth (ΔH) narrows as x increases up to $x \sim 0.03$, due to exchange narrowing.

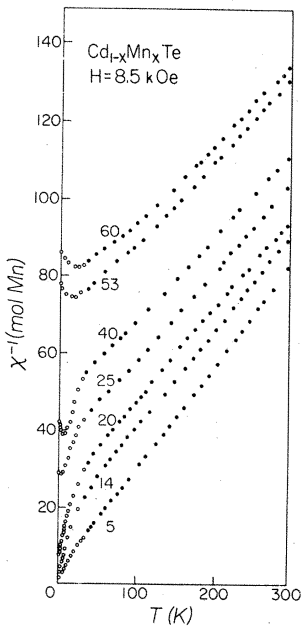

FIG. 1. χ^{-1} of $Cd_{1-x}Mn_xTe$. The low-temperature data (open circles) were taken after ZFC for increasing T. The high-temperature data (full circles) were obtained after FC for decreasing T.

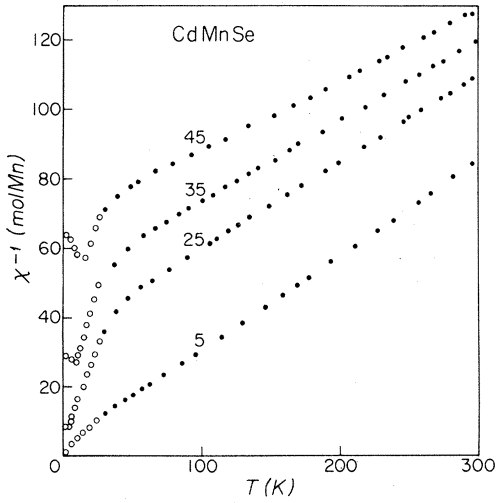

FIG. 2. χ^{-1} of $Cd_{1-x}Mn_xSe$ for 5, 25, 35, and 45 at. % of Mn. The low-temperature data (open circles) were taken after ZFC for increasing T in a 30-Oe field. The high-temperature data (full circles) were obtained in an $H=8.5$-kOe field.

For $x>0.03$ ΔH broadens monotonically with increasing concentration at all temperature measured. A significant increase in ΔH with decreasing T is observed for all samples with $x>0.03$. The observed linewidths as a function of T and x are given in Figs. 5 and 6.

A shift with T of the resonance field (H_R) of the EPR line was observed for $0.10\leq x\leq 0.15$ and $0.15\leq x\leq 0.25$ for $Cd_{1-x}Mn_xTe$ and $Cd_{1-x}Mn_xSe$, respectively. For other values of x, changes in the position of the line could not be observed because (a) at lower values of x we were limited by our lowest available T, ~ 1.5 K, and (b) at higher concentrations ΔH was too large to be measured even at high T. The observed change in the position of the resonance line $H_i=H_0-H_R$, where H_0 is the magnetic field corresponding to a gyromagnetic factor $g=2$, is shown in Fig. 7 as a function of T, ν, and x.

C. Remanent magnetization

One set of data for the remanent magnetization (M_R) was obtained by using the EPR technique described in Sec. II. The M obtained from the splitting between the two EPR marker signals range from 10 to 50 Oe, depending on x. The M vs T curves (not shown) obtained for different x are in agreement with the curves obtained using

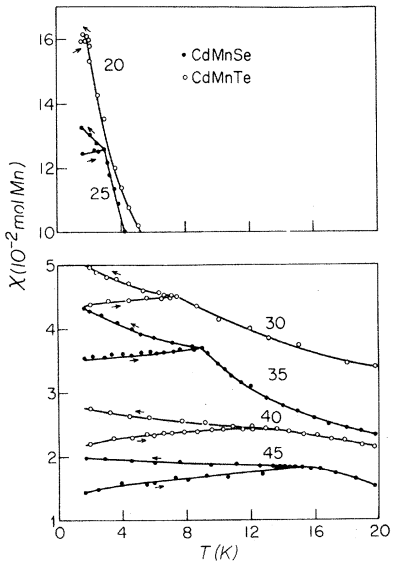

FIG. 3. ZFC and FC χ data of $CD_{1-x}Mn_xSe$ (25, 35, and 45 at. % of Mn) and $Cd_{1-x}Mn_xTe$ (20, 30, and 40 at. % of Mn) as a function of T near T_f in an $H=30$-Oe field. The arrows indicate the two cases.

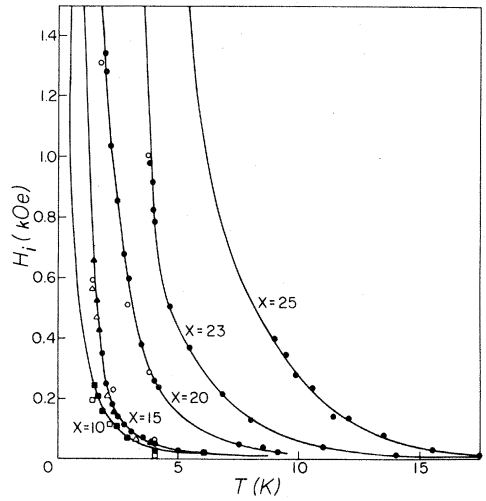

FIG. 7. Temperature dependence of the internal magnetic field H_i for $Cd_{1-x}Mn_xSe$, $x=15$, 20, 23, and 25 at. %, at 9 GHz (full circles) and at 35 GHz (open circles); for $Cd_{0.90}Mn_{0.10}Te$ at 9 GHz (full squares) and 35 GHz (open squares), and for $Cd_{0.85}Mn_{0.15}Te$ at 9 GHz (full triangles) and 35 GHz (open triangles). Solid lines are least-squares fits to the data with values shown in Tables I and II using Eq. (3). H_i is defined as $H_i=H_0-H_R$, where H_0 is the field corresponding to $g=2$ and H_R the measured resonance field.

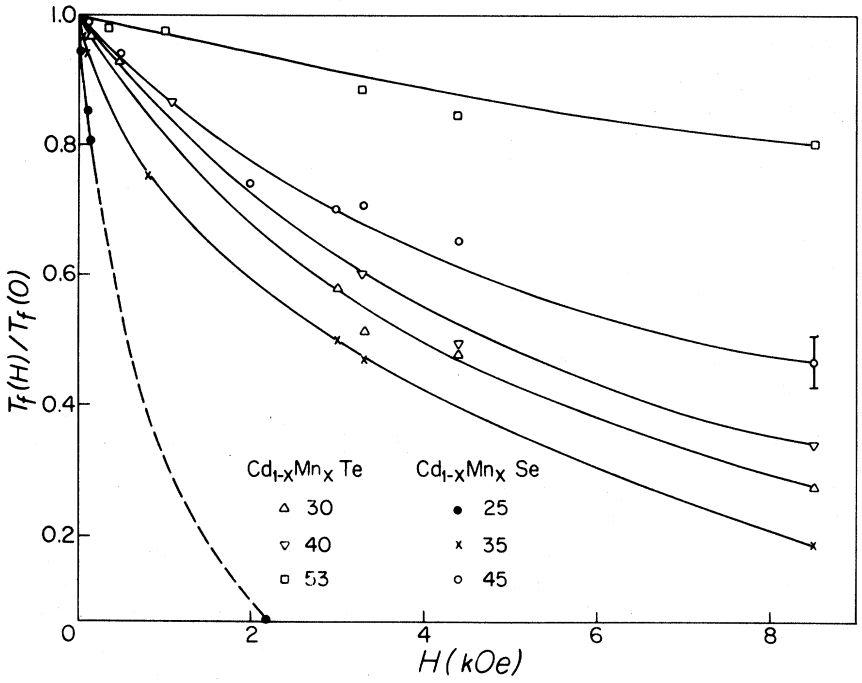

FIG. 4. Observed $T_f(H)/T_f(0)$ ratio as a function of H; $T_f(H)$ is the temperature at which χ shows a maximum at a given H, measured after ZFC. The dashed curves give the field for which $T_f(H)=0$, and was obtained from the coincidence of the σ and σ' curves.

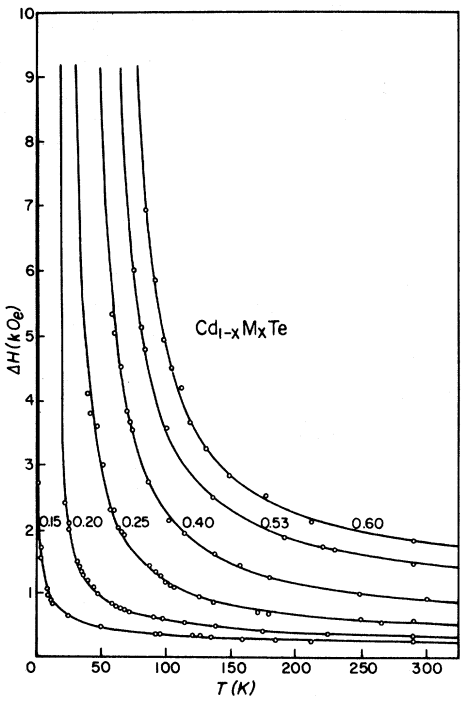

FIG. 5. Temperature dependence of the peak-to-peak EPR linewidth for $Cd_{1-x}Mn_xTe$ ($0.05 \leq x \leq 0.60$). The solid lines are least-squares fits to the data with values shown in Table II using Eq. (2).

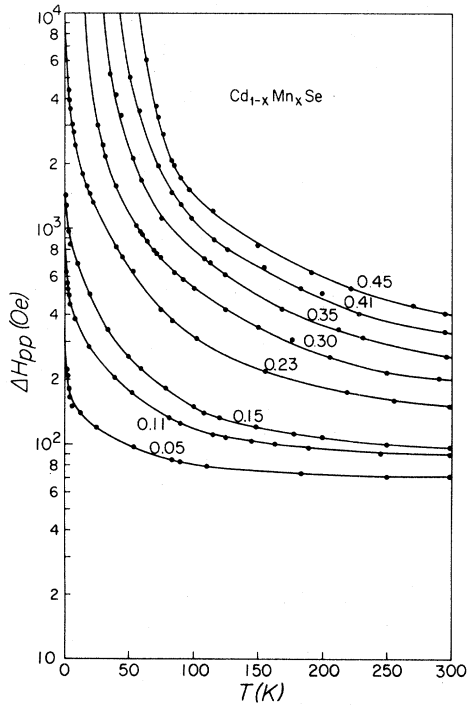

FIG. 6. Temperature dependence of the peak-to-peak EPR linewidth for $Cd_{1-x}Mn_xSe$ ($0.05 \leq x \leq 0.45$). Solid lines are least-squares fits to the data with values shown in Table I using Eq. (2).

the Faraday method. The values of T_f thus obtained are included in Fig. 4.

Using this technique we measured the increase and decay of the ZFC isothermal remanent magnetization (σ) and the FC thermoremanent magnetization (σ') for $0.40 \leq x \leq 0.60$ in $Cd_{1-x}Mn_xTe$ and $0.35 \leq x \leq 0.45$ for $Cd_{1-x}Mn_xSe$. Figure 8 illustrates how these experiments were performed.

The increase (i) of σ was obtained by cooling the sample to $T < T_f$ at zero field, then the resonance field, ~ 3.3 kOe, was applied and the splitting δH of the two EPR silicon markers measured as a function of t. σ_i is then defined by

$$\sigma_i = \delta H_{\mathrm{ZFC}}(H,t) - \delta H'_{\mathrm{ZFC}}(H, t = 25 \text{ s}) , \qquad (1)$$

$\delta H_{\mathrm{ZFC}}(H,t)$ being the splitting measured after ZFC at a time t after the field was turned on, and $\delta H'_{\mathrm{ZFC}}(H,t=25$ s) the splitting for $t = 25$ s, which is the shortest time in which we could take a resonance spectrum. We also measured the decay (d) of σ, defined as

$$\sigma_d = \delta H_{\mathrm{ZFC}}(H, \tau_1 \rightarrow \infty) - \delta H'_{\mathrm{ZFC}}(H, \tau_2, t = 25 \text{ s}) ,$$

where $\delta H_{\mathrm{ZFC}}(H, \tau_1 \rightarrow \infty)$ indicates the splitting after ZFC before applying the resonance field for a long time ($\tau_1 \rightarrow \infty$). $\delta H'_{\mathrm{ZFC}}(H, \tau_2, t = 25$ s) indicates the splitting measured after the last state is obtained, the field is then turned off for different times $t = \tau_2$ before the field is finally applied for just 25 s. In a similar way we measured σ'_i and σ'_d in FC samples.

The values of the increase and decay of σ and σ' are given for $Cd_{0.60}Mn_{0.40}Se$ in Fig. 9. Values of

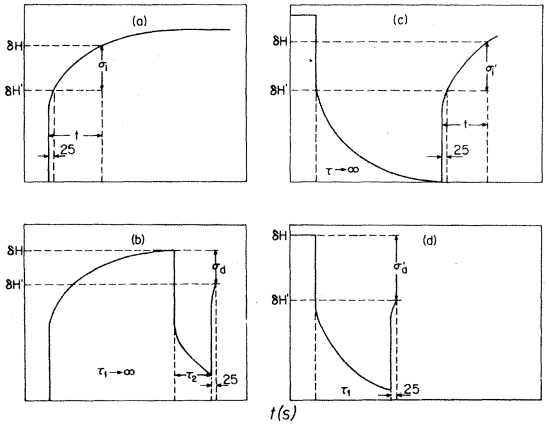

FIG. 8. Sketch of the way that the increase (i) and decay (d) of the thermoremanent magnetization (σ') and isothermal remanent magnetization (σ) were obtained by measuring δH, the separation of the two EPR marker signals as a function of time.

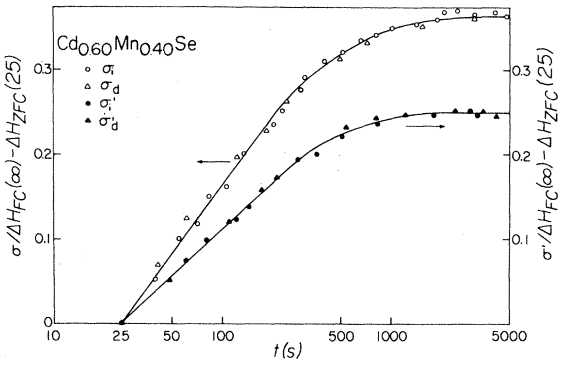

FIG. 9. EPR measurements of the increase and decay of σ and σ' as a function of t for $Cd_{0.60}Mn_{0.40}Se$ at 4 K.

σ_i as a function of t and T are given in Figs. 10 and 11. In Figs. 9–11, σ and σ' are normalized to the difference in splitting of $\delta H_{\mathrm{FC}}(H, t = \infty)$ and $\delta H_{\mathrm{ZFC}}(H, t = 25$ s), the two extremes of our data. The total change of the splitting was of several linewidths, which allowed us to obtain σ and σ' with a small error.

Using the vibrating sample magnetometer we obtained the field dependence of σ_d and σ'_d. To measure the field dependence of σ_d, we carried out the following procedure: After ZFC the sample to a given $T < T_f$, a field H was applied for a certain time, and σ_d was measured 30 s after the field was turned off. This procedure was repeated for different values of H. To measure σ'_d we FC the sample for different values of H to $T < T_f$ and measured σ'_d 30 s after switching off the field. The field dependence of σ and σ' for $Cd_{0.75}Mn_{0.25}Se$ is given in Fig. 12; similar data were obtained for different x in both systems. We have also studied the time dependence of σ'_d for

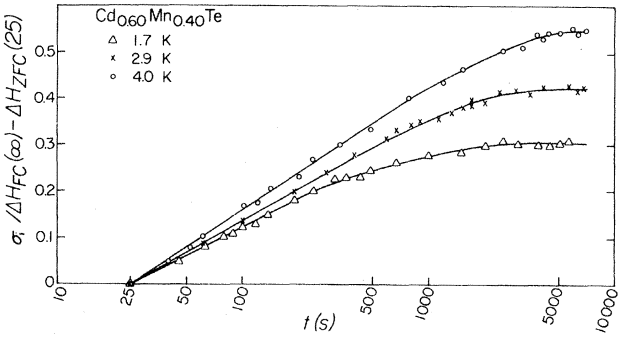

FIG. 10. σ_i as a function of t for $Cd_{0.60}Mn_{0.40}Te$ for different T measured by EPR.

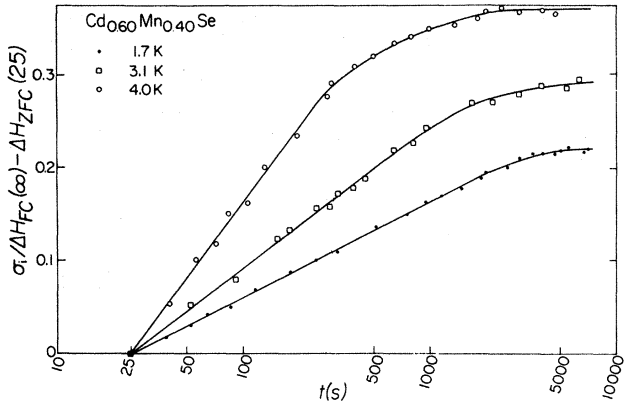

FIG. 11. σ_i as a function of t for $Cd_{0.60}Mn_{0.40}Se$ for different T measured by EPR.

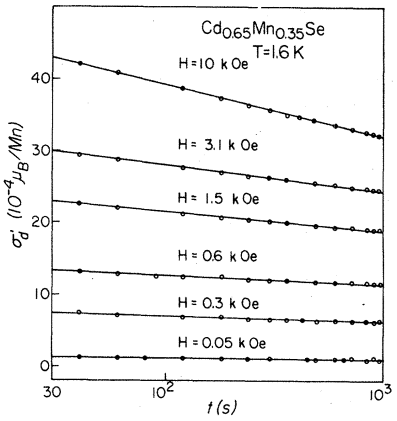

FIG. 13. Time and field dependence of σ'_d for $Cd_{0.65}Mn_{0.35}Se$ at 1.7 K.

fixed values of T and H. Typical data can be observed in Fig. 13. The value of the magnetic field H'_K, where the curves of σ_d and σ'_d tend to coincide increases with x, as shown in Table I.

IV. ANALYSIS

A. dc susceptibility

The dc susceptibility for $Cd_{1-x}Mn_xTe$ and $Cd_{1-x}Mn_xSe$ shows a similar behavior over the entire concentration range studied. For T above ~ 50 K, all the samples analyzed obey a Curie-Weiss law $\chi^{-1}_{\text{mol Mn}} = T - \Theta/C$ as shown in Figs. 1 and 2. The values obtained for the Curie constant C and the asymptotic Curie temperature Θ as a function of x are shown in Figs. 14(a) and (b), and listed in Tables I and II. For $x < 0.04$ the extrapolation of the linear portion of χ^{-1} intersects the positive T axis, implying that at low Mn concentration the predominant interaction is ferromagnetic. For both systems, Θ showed a maximum of ~ 10 K at $x \simeq 0.02$. For $x > 0.04$, χ^{-1} intersects the negative T axis, implying that in this region the dominant interactions are AF.

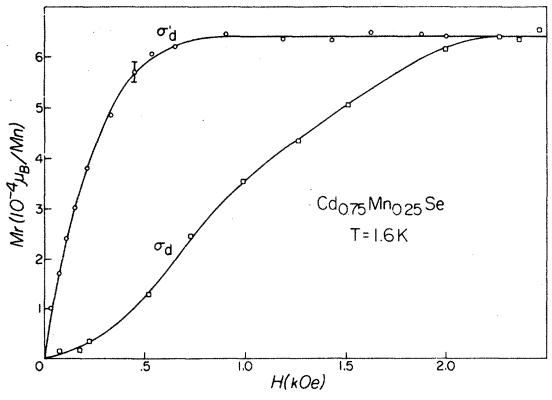

FIG. 12. Field dependence of σ_d and σ'_d for $Cd_{0.75}Mn_{0.25}Se$ at 1.6 K.

As seen in Figs. 1 and 2, for T below 50 K and $x < 0.20$, the curves χ^{-1} vs T show a continuous downturn towards the origin. At low x this magnetic behavior can be analyzed in terms of a cluster model.[13] In our case, this model explains only qualitatively the downturn towards the origin of χ^{-1}. For a better fit of the data, a larger number of clusters were necessary than statistically predicted.[14] For example, for $x \simeq 0.01$ the best fit was obtained by using 30% of pairs instead of the 14% which would follow from a random distribution. The deviation from a random distribution became larger as we increased x. This behavior was also observed by Galazka *et al.*[9]

For $x \gtrsim 0.20$, when the sample was ZFC, a maximum in χ was observed at a temperature T_f. The position of the maximum for $H \to 0$ was obtained by extrapolating to zero field the values of the peak position $T_f(H)$ for fields ranging from 8.5 kOe to 30 Oe as shown in Fig. 4. The values thus obtained are given in Tables I and II and shown in Fig. 14(c). A linear extrapolation of $T_f(H \to 0)$ intersects the concentration axis at $x \simeq 0.17$ for $Cd_{1-x}Mn_xTe$ and at $x \simeq 0.20$ for $Cd_{1-x}Mn_xSe$ as shown in Fig. 14(c). According to the theory of

TABLE I. Values as a function of concentration for $Cd_{1-x}Mn_xSe$ of: the Curie temperature Θ, the Curie constant C, the extrapolated temperature for the maximum of χ, $T_f(H\rightarrow 0)$ after zero-field cooling, the temperatures $T_{f\Delta H}$ and T_{fH_i} and critical exponents $\alpha_{\Delta H}$ and α_{H_i} obtained from the temperature dependence of the EPR linewidth and the internal magnetic field H_i measured from the shift of the EPR line, the effective concentration x^* obtained from $x^*=xM(x)/M$ ($x=5$ at. %), the mean anisotropy field H_K obtained from Eq. (3), and the mean anisotropy field H_K' obtained from the coincidence of the σ and σ' curves.

$x(\pm 1)$ (at. %)	$-\Theta(\pm 10)$ (K)	$C(\pm 0.1)$ $\left[\frac{\text{K cm}^3}{\text{mol Mn}}\right]$	$T_f(H\rightarrow 0)$ (K)	$T_{f\Delta H}$ (K)	T_{fH_i} (K)	$\alpha_{\Delta H}(\pm 0.2)$	$\alpha_{H_i}(\pm 0.5)$	x^* (at. %)	$H_K(\pm 25\%)$ (kOe)	$H_K'(\pm 10\%)$ (kOe)
1	−3	3.85								
2	−10	3.75								
5	10	3.65	$<<1$	$<<1$		0.2		5		
11				$<<1$		0.3				
15	80	4.05	$<<1$	$<<1$	~0.2	0.4	2.2	3.3		
20				~0.3	~0.3	0.5	2.9			
23	120	4.1	1.8±0.5	~1	~0.4	0.6	3.2			
25	135	4.1	3.0±0.5	~1	~1	1.0	5.4	2.7	2	2.2
30				3.5±1		1.3				
35	220	4.35	9.3±1	6±1		1.8		1.6	11	13
41				9±1		1.9				
45	330	4.90	15±2	11.5±1		2.0		1.2	21	

the site percolation problem, the mean cluster becomes infinite at the critical concentration x_c. When only nearest neighbors are considered, a value of $x_c\simeq 0.195$ is obtained for an fcc lattice.[15,16] For an hcp lattice, a value of $x_c\simeq 0.204$ has been reported.[16] The close agreement between the calculated values for x_c and the lowest x, where the maximum in χ vs T appears experimentally at $H\rightarrow 0$, suggests a correlation between the appearance of the peak and the percolation critical point x_c.

As seen in Fig. 4, when H was increased, the

TABLE II. Values as a function of concentration for $Cd_{1-x}Mn_xTe$ of: the Curie temperature Θ, the Curie constant C, the extrapolated temperature for the maximum of χ, $T_f(H\rightarrow 0)$ after zero-field cooling, the temperatures $T_{f\Delta H}$ and T_{fH_i} and critical exponents $\alpha_{\Delta H}$ and α_{H_i} obtained from the temperature dependence of the EPR linewidth and the internal magnetic field H_i measured from the shift of the EPR line, the effective concentration x^* obtained from $x^*=xM(x)/M$ ($x=5$ at. %), and the mean anisotropy field H_K obtained from Eq. (3).

$x(\pm 1)$ (at. %)	$-\Theta(\pm 10)$ (K)	$C(\pm 0.1)$ $\left[\frac{\text{K cm}^3}{\text{mol Mn}}\right]$	$T_f(H\rightarrow 0)$ (K)	$T_{f\Delta H}$ (K)	T_{fH_i} (K)	$\alpha_{\Delta H}(\pm 0.2)$	$\alpha_{H_i}(\pm 0.5)$	x^* (at. %)	$H_K(\pm 25\%)$ (kOe)
1	−5	4.0							
2	−10	3.9							
5	2	3.85	$<<1$	0.01		0.3		5	
10	35			0.35	0.05	0.4	1.7		
15	70	4.10	$<<1$	0.85	0.2	0.5	2.2	3.2	
20	100	4.35	2±0.5	4±2		0.6		2.6	
30	170	4.40	9±1	9±2		1.5		1.5	14
40	230	4.60	15±2	13±3		1.5		1.3	19
53	310	4.55	18±2	20±3		1.6		1.2	75
60	350	4.60	23±3	25±3		1.5		1.1	

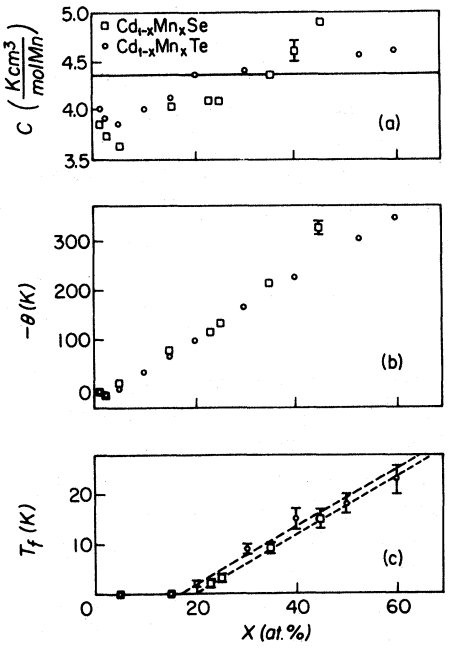

FIG. 14. Concentration dependence for both systems for (a) the Curie constant C where the value of the free ion $C=4.375$ K cm^3/mol Mn is given for comparison, (b) the Curie temperature Θ, and (c) the extrapolated value at $H\rightarrow 0$, for the maximum observed at $T_f(H\rightarrow 0)$ for χ after ZFC.

maximum in χ shifted to lower T and became weaker and broader. Wohlforth[17] has analyzed this effect in spin-glasses, proposing that they exhibit rock magnetism. In terms of the Neel's model,[18] the following approximate relation can be written:

$$\left[\frac{T_f(H)}{T_f(0)}\right]^{1/2}=1-\frac{H}{H_K}\ , \tag{3}$$

where $T_f(H)$ is the position of the maximum of χ measured in a field H, $T_f(0)$ is the extrapolated peak position at zero field, and H_K is the mean anisotropy field of the cluster. Values of H_K obtained by comparing our data with Eq. (3) are given in Tables I and II. The fit of our data to Eq. (3) is shown in Fig. 15. H_K can be obtained independently from the coincidence of the ZFC isothermal remanent magnetization (σ) and the FC thermoremanent magnetization (σ') curves.[17] Values of H_K obtained by the two methods are in good agreement, as shown in Table I.

In the case of dilute canonical spin-glass systems, such as *Cu*Mn and *Au*Fe, the reduced properties [$M(H,T)/x$, $C_p(H,T)x$, etc.] can be described by universal functions of H/x and T/x.[19] These scaling laws are no longer obeyed in our systems. However, M can be scaled upon a universal curve for a given T/x for all the investigated fields, as shown in Figs. 16 and 17, where the data are all brought into coincidence with the M of $x=5\%$ by scaling factors given by $x^*=xM(x)/M(x=5\%)$. The values of x^* are shown in Tables I and II and in the insets of Figs. 16 and 17, as a function of x. The observed universality of the M allows us to write the new scaling law, $M/x^*=f(T/x,H/x)$, by substituting M/x for M/x^*. A similar behavior has been ob-

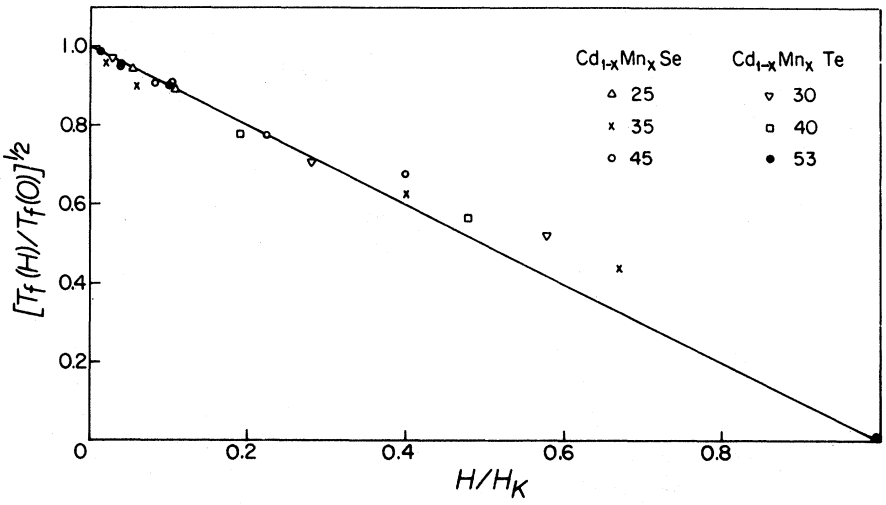

FIG. 15. Fit of the $T_f(H)$ data to Eq. (3).

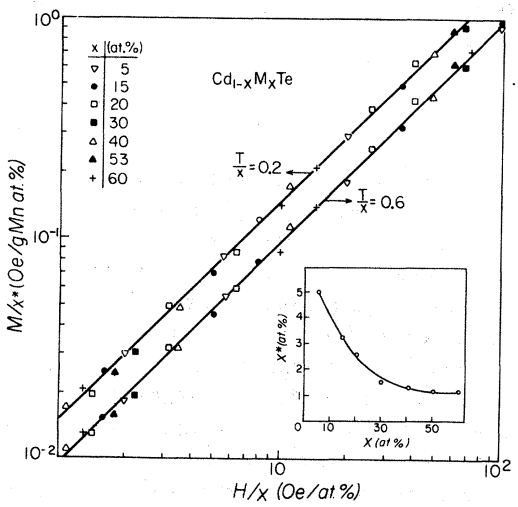

FIG. 16. Modified reduced magnetization M/x^* as a function of reduced magnetic field H/x for $Cd_{1-x}Mn_xTe$ at two different reduced temperatures T/x. The inset shows the scaling concentration x^* as a function of the real concentration x.

served in other concentrated systems.[20–22] Using the C_p data reported for $Cd_{1-x}Mn_xTe$,[9] we found scaling factors for $x=0.10$, 0.20, and 0.30 in fair agreement with those listed in Table I. Thus, in principle, a scaling law similar to M can be expected for C_p.

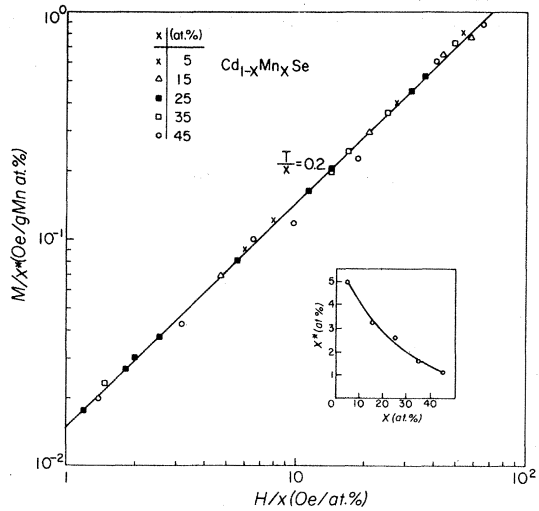

FIG. 17. Modified reduced magnetization M/x^* as a function of reduced magnetic field H/x for $Cd_{1-x}Mn_xSe$ at $T/x=0.2$. The inset shows the scaling concentration x^* as a function of the real concentration x.

B. EPR

Our data on the EPR spectra at low concentrations, $x<0.005$, give values of the parameters for the spin-Hamilitonian in good agreement with previous results.[11,12] The observed broadening of ΔH for $x>0.03$ with decreasing T can be described using the modified Huber expression,[23,24]

$$\Delta H_{pp}=A\left[\frac{T_{f\Delta H}}{T-T_{f\Delta H}}\right]^{\alpha_{\Delta H}}+B\left[\frac{\Theta}{T}+1\right], \quad (4)$$

where ΔH_{pp} denotes the peak to peak EPR linewidth, A and B are suitable constants to be obtained from the experiment, $\alpha_{\Delta H}$ is the critical exponent, $T_{f\Delta H}$ is the T of the order-disorder transition, and $B(\Theta/T+1)$ is the high-T linewidth. The first term on the right accounts for the dynamical contribution and is valid only for T close to $T_{f\Delta H}$; the second term becomes dominant for $T>>T_{f\Delta H}$ and it explains the decrease of ΔH as T increases in a region that bears no relation with the critical phenomena.

The observed shift of H_R with T for the EPR line was independent, within the experimental error, of the microwave frequency used. It can be attributed to an internal field $H_i=H_0-H_R$ that is built up as we approach the transition temperature T_{fH_i}, and not to a change in the gyromagnetic factor (if that was the case, the shift of H_R would be proportional to ν).

The increase of H_i with decreasing T can be analyzed with an expression similar to Eq. (4), where the second term on the right, which accounts for H_i at high T, is taken equal to zero. We can then write

$$H_i=A'\left[\frac{T_{fH_i}}{T-T_{fH_i}}\right]^{\alpha_{H_i}}, \quad (5)$$

where T_{fH_i} is the transition T obtained from the change of H_R and A' a constant to be obtained from the experiment.

Since Eqs. (4) and (5) are expected to be valid near the transition, the values of $T_{f\Delta H}$, T_{fH_i}, $\alpha_{\Delta H}$, and α_{H_i} listed in Tables I and II were obtained using only the low-T data. The solid lines in Figs. 5–7 are a least-squares fit of the experimental values with Eqs. (4) and (5).

From the parameters listed in Tables I and II, we can separate our EPR results into three regions of the concentration: $x<0.15$, $0.15\lesssim x\lesssim 0.20$, and

$x > 0.20$ for $Cd_{1-x}Mn_xTe$ and $x < 0.20$, $0.20 \lesssim x \lesssim 0.25$, and $x > 0.25$ for $Cd_{1-x}Mn_xSe$. For the region of high x, the values obtained for $T_{f\Delta H}$ are in good agreement with those that follow from dc measurements at the same field. In this region, we found that $T_{f\Delta H}$ became substantially larger than for the low-x region, increasing linearly with x as listed in Tables I and II.

The transition from the low values of $T_{f\Delta H}$ in the region of lowest x to larger and linearly dependent values of $T_{f\Delta H}$ in the region of largest x occurs between $0.15 < x < 0.20$ and $0.20 < x < 0.25$ for $Cd_{1-x}Mn_xTe$ and $Cd_{1-x}Mn_xSe$, respectively. The calculated x_c and our extrapolated lowest x for $T_f \neq 0$ at 3.3 kOe obtained from the χ data both fell into the corresponding region for each system. This shows an agreement between the data obtained by EPR and dc susceptibility and the calculated x_c for the site percolation problem.

C. Remanent magnetization

The results of the analysis of the M_R data obtained by both techniques can be summarized as follows: (i) The time dependence can be fitted by a $\log(t)$ law over the first two to three decades ($t < 1000$ s), i.e., $M_R = M_0 \pm S \log t$; (ii) at 3.3 kOe the coefficient S_σ is larger than $S_{\sigma'}$ as seen in Fig. 9, a behavior observed before[25]; (iii) S_σ and $S_{\sigma'}$ are the same for the increase and decay of M_R as shown in Fig. 9; (iv) S_σ increases with T as is shown in Figs. 10 and 11; (v) $S_{\sigma'}$ increases as H increases, which explains why Galazka *et al.*[9] were not able to observe any relaxation when they measured $Cd_{1-x}Mn_xTe$ at low field, and (vi) the field dependence of σ and σ' is similar to that found in other spin-glasses, except that a broad maximum at σ' did not show up in our materials, as seen in Fig. 12.[25–27]

V. DISCUSSION AND CONCLUSIONS

The magnetic susceptibility and EPR data presented in this work indicate that $Cd_{1-x}Mn_xTe$ and $Cd_{1-x}Mn_xSe$ have a similar magnetic behavior which changes at a concentration close to the percolation threshold x_c calculated for nearest neighbors. The data is then separated into two concentration regions below and above x_c.

For $x < x_c$, both systems remain paramagnetic for all T measured. The value of Θ obtained from χ at high T when introduced into expression (4) accounts for the decrease of the EPR linewidth as T increases, indicating an agreement between the data obtained by EPR and χ at low x and high T. The downturn of χ at low T along with the broadening and shift of H_R of the EPR line can be understood qualitatively by the increase of an internal field due to the presence of finite clusters. However, to fit the χ data, a larger number of clusters was necessary than statistically predicted. This behavior should be related to the fact that the method used to obtain the single crystals requires a slow cool-down after the compound is melted which favors the formation of Mn clusters. It would then be of interest to measure the samples after treating them in different ways to try to reduce the presence of nonstatistically Mn clusters (for example, by annealing them at different temperatures and times before quenching them in water).

For a zinc-blende structure, which is the case in $Cd_{1-x}Mn_xTe$, the next-nearest-neighbor interaction between the Mn ions is expected to be much smaller than the nearest-neighbor interaction.[28] Under these conditions De Seze[6] suggested that for $x > x_c$, a spin-glass phase becomes favorable at low T due to frustration of the AF interactions. A similar behavior can be expected for the $Cd_{1-x}Mn_xSe$ structure. In effect the data on these systems, for $x > x_c$, exhibit several magnetic properties indicative of a spin-glass transition, such as a maximum in the low-field χ when ZFC and a time-dependent remanent part of M below T_f.

The T dependence of the maximum with x and H is similar to other systems showing a spin-glass behavior. T_f was observed to be a linear function of x when measured at low field. The field dependence of T_f can be interpreted in terms of Neel's model of superparamagnetism. From this analysis, mean values of the anisotropy field H_K were estimated. An independent estimate of H_K was obtained from the field where the thermoremanent and isothermal remanent magnetizations coincided. Both values of H_K agree where there is an overlap as shown in Table I. The values obtained for T_f from χ and EPR when measured at the same field agree well, showing also at this concentration range an agreement between the results obtained from both techniques.

The time-dependent remanent part of M has a similar behavior as in other metallic and nonmetallic spin-glasses. The faster relaxation rate of σ with respect to σ', the increase of S_σ and $S_{\sigma'}$ with T, and the increase of $S_{\sigma'}$ under larger magnetic

fields, are in agreement with recent calculations.[29,30]

The fact that these systems present spin-glass properties at high x explains why M was not found to follow the scaling law obeyed by diluted spin-glasses. However, the M can be scaled upon a universal curve by substituting M/x with M/x^*. In a crude model we can visualize these concentrated materials as nonoverlapping rigid antiferromagnetic clusters considered as individual entities interacting via random forces. The average number of spins of each cluster is not constant, but increases with x, as can be seen from the ratio x/x^* given in Tables I and II.

We conclude that $Cd_{1-x}Mn_xTe$ and $Cd_{1-x}Mn_xSe$, aside from unsolved metallurgical problems that result in nonstatistical Mn clusters and the scaling law not obeyed for M, present magnetic properties similar to those of other metallic and nonmetallic systems known as spin-glasses. So, in principle, these materials behave according to the original suggestion of De Seze about the existence of an insulating spin-glass with purely AF interactions. However, to have a more complete picture of the magnetic behavior of these systems it would be convenient to measure the ac susceptibility to obtain the ν dependence of T_f, and to perform neutron diffraction measurements where the high neutron absorption cross section of Cd can be highly reduced by eliminating the isotope Cd^{113}.

ACKNOWLEDGMENTS

I wish to thank Professor W. Giriat for supplying the crystals. I gratefully acknowledge the generous help with the experimental work given by Dr. F. Acker, Dr. R. Calvo, and Dr. Z. Fisk. It is also a pleasure to acknowledge useful advice and encouragement from Professor S. Shultz, as well as the stimulating copy of his manuscript[10] received prior to publication. I am grateful to Professor J. Fernández for a critical reading of the manuscript and for his valuable comments and discussions during the course of this work. This research was supported in part by Consejo Nacional de Investigaciones Cieutificas y Tecnicas, Venezuela.

[1]J. A. Mydosh, in *Proceedings of the Second International Symposium on Amorphous Magnetism, Troy, 1976,* edited by R. A. Levy and R. Hasegawa (Plenum, New York, 1977).
[2]K. H. Fischer, Physica (Utrecht) 86-88, 813 (1976).
[3]V. Cannella and J. A. Mydosh, Phys. Rev. B 6, 4220 (1972).
[4]P. W. Anderson, in *Ill-Condensed Matter, Les Houches, 1978,* edited by R. Balian, R. Maynard, and G. Toulouse (North-Holland, Amsterdam, 1979).
[5]J. Kondo, Prog. Theor. Phys. 33, 575 (1965).
[6]L. De Seze, J. Phys. C 10, L353 (1977).
[7]J. Villain, Z. Phys. B 33, 31 (1979).
[8]S. Oseroff and F. Acker, Solid State Commun. 37, 19 (1981).
[9]R. R. Galazka, S. Nagata, and P. H. Keesom, Phys. Rev. 22, 3344 (1980).
[10]S. Shultz, E. M. Gullikson, D. R. Fredkin, and M. Tovar, Phys. Rev. Lett. 45, 1508 (1980).
[11]J. Schneider, S. R. Sirear, and A. Rauber, Z. Naturforsch. 18A, 980 (1963).
[12]J. Lambe and C. Kikuchi, Phys. Rev. 119, 1256 (1960).
[13]A. W. Simpson, Phys. Status Solidi B 40, 207 (1970).
[14]M. M. Kreitman and D. L. Barnett, J. Chem. Phys. 43, 364 (1965).
[15]C. Domb and N. W. Dalton, Proc. Phys. Soc. London 89, 859 (1966).
[16]H. L. Frisch, E. Sonnenblick, V. A. Vyssotsky, and J. M. Hammersley, Phys. Rev. 124, 1021 (1961).
[17]E. P. Wohlfarth, J. Phys. F 10, L241 (1980).
[18]L. Neel, Ann. Geophys. 5, 99 (1949).
[19]A. Blandin, J. Phys. (Paris) 39, C6-1499 (1978).
[20]S. J. Poon and J. Durand, Phys. Rev. 18, 6253 (1978).
[21]D. Krischel and L. K. Thomas, J. Phys. F 10, 115 (1980).
[22]J. J. Smit, G. J. Nieuwenhuys, and L. J. de Jongh, Solid State Commun. 31, 265 (1979).
[23]D. L. Huber, Phys. Rev. B 6, 3180 (1972).
[24]E. Dormann and V. Jaccarino, Phys. Lett. A 48, 81 (1974).
[25]J. Ferre, J, Rajchenbach, and H. Maletta, J. Appl. Phys. (in press).
[26]H. Maletta and W. Felsch, Phys. Rev. B 20, 1245 (1979).
[27]J. L. Tholence and R. Tournier, J. Phys. (Paris) 35, C4-229 (1974).
[28]W. H. Brumage, C. R. Yager, and C. C. Lin, Phys. Rev. 133, A 765 (1964).
[29]W. Kinzel, Phys. Rev. B 19, 4595 (1979).
[30]C. H. Dasgupta, S. Ma, and Ch. Hu, Phys. Rev. B 20, 3837 (1979).